ENHANCED PHASE STABILITY OF METASTABLE TETRAGONAL ZIRCONIA NANOCRYSTALS PREPARED THROUGH NOVEL CHEMICAL ROUTES

A THESIS SUBMITTED IN PARTIAL FULFILLMENT
OF THE REQUIREMENTS FOR THE DEGREE OF

Bachelor of Technology
in
Ceramic Engineering

By

NABID ANJUM KHAN

Department of Ceramic Engineering
National Institute of Technology
Rourkela
2007

ENHANCED PHASE STABILITY OF METASTABLE TETRAGONAL ZIRCONIA NANOCRYSTALS PREPARED THROUGH NOVEL CHEMICAL ROUTES

A THESIS SUBMITTED IN PARTIAL FULFILLMENT
OF THE REQUIREMENTS FOR THE DEGREE OF

Bachelor of Technology
in
Ceramic Engineering

By
NABID ANJUM KHAN

Under the Guidance of
Prof. Bibhuti B. Nayak

Department of Ceramic Engineering
National Institute of Technology
Rourkela
2007

National Institute of Technology

Rourkela

CERTIFICATE

This is to certify that the thesis entitled, "ENHANCED PHASE STABILITY OF METASTABLE TETRAGONAL ZIRCONIA NANOCRYSTALS PREPARED THROUGH NOVEL CHEMICAL ROUTES" submitted by Sri Nabid Anjum Khan in partial fulfillments for the requirements for the award of Bachelor of Technology Degree in Ceramic Engineering at National Institute of Technology, Rourkela (Deemed University) is an authentic work carried out by him under my supervision and guidance.

To the best of my knowledge, the matter embodied in the thesis has not been submitted to any other University / Institute for the award of any Degree or Diploma.

Date:

Prof. Bibhuti B. Nayak
Dept. of Ceramic Engineering
National Institute of Technology
Rourkela - 769008

ACKNOWLEDGEMENT

I wish to express my deep sense of gratitude and indebtedness to Prof. Bibhuti B. Nayak, Department of Ceramic Engineering, N.I.T Rourkela for introducing the present topic and for their inspiring guidance, constructive criticism and valuable suggestion throughout this project work.

I would like to express my gratitude to Prof. S. Bhattacharyya (Head of the Department), Prof. S. Adak, Prof. J. Bera, Prof. S. K. Pratihar, Prof. D. Sarkar and Prof. A. Mallik for their valuable suggestions and encouragements at various stages of the work. I am also thankful to all staff members of Department of Ceramic Engineering NIT Rourkela.

I am grateful to Prof. U. K. Mohanty Department of Metallurgical and Materials Engineering for helping us for doing measurements in their department. I am also thankful to Mr. Uday, Mr. Sameer and Mr. Rajesh for doing DSC-TG and SEM measurements of our samples.

I am also grateful to Dr. A. Mondal, (Scientist, RRL Trivandrum) for helping us for doing IR measurement and analysis of our samples.

I am also thankful to Mr. R. P. Rana and Mr. Y. Nayak and other research scholars in Department of Ceramic Engineering for providing all joyful environment in the lab and helping me out in different ways.

I feel a deep sense of gratitude for my father Mr. Liakat Ali Khan and mother Kamrun Nisha who formed a part of my vision and taught me the good things that really matter in life. I would like to thank my brothers, sisters other family members for their support.

Last but not least, my sincere thanks to all my friends who have patiently extended all sorts of help for accomplishing this undertaking.

30th April 2007 (NABID ANJUM KHAN)

CONTENTS

ABSTRACT

The present work deals with the synthesis and enhancement of metastable tetragonal zirconia nanocrystals through novel chemical routes. Nanocrystalline t-ZrO_2 is a technologically significant material that finds extensive use as catalyst or catalyst support, oxygen sensor and structural components.

In this work, ZrO_2 nanoparticles are synthesized using both reduction and hydrolysis techniques. These techniques are known to result in the production of nanocrystalline materials. Also, promote the stabilization of t-phase of ZrO_2 at the nano level at moderate temperature, which is one of the primary objective of this work.

For reduction technique, the Zr-salts are reduced by the addition of strong (Sodium borohydride, $NaBH_4$) and weak (Hydrazine hydrate, N_2H_5OH) reducing agents. However for hydrolysis technique, Zr-salts are hydrolyzed by adding ammonium hydroxide (NH_4OH). In this process, geletion and precipitation occurred at low and high pH respectively with the addition of these agents. Here, the main objective is to stabilize the t-ZrO_2 through geletion (low pH) and precipitation (high pH) route by using $NaBH_4$ and N_2H_5OH and compare with the powders synthesized through hydrolysis process by the addition of NH_4OH. It was observed that the crystallization temperature of t-ZrO_2 for low pH is greater as well as broad range than the high pH ZrO_2 samples. Stabilization of metastable t-ZrO_2 is observed up to 600 °C for both pH in case of samples reduction by $NaBH_4$. Stabilization of metastable t-ZrO_2 is observed up to 500 °C for low pH in case of samples reduction by N_2H_5OH. Fully t-ZrO_2 is seen for low pH sample, however mixture of t- and m- ZrO_2 are observed for high pH sample up to 500 °C for the case of NH_4OH. The as-prepared powders contain lots of water in the form of $ZrO(OH)_2.xH_2O$ as studied from the IR analysis. From the XRD results it has been concluded that small crystallites (<25nm) stabilizes metastable t-ZrO_2 upto moderate temperature. Low pH has better stability on metastable t-ZrO_2 compared to high pH. Strong reducing agent ($NaBH_4$) gives better stability on t-ZrO_2 upto 600 °C compared to NH_4OH. Reduction technique controls the crystallite size and slowly converts to m-ZrO_2 as the calcination temperature increases.

From the thermal as well as microstructural studies it was concluded that the stabilization of t-ZrO_2 is dependent on the initial pH of the precursor, calcination temperature and also on the crystallite size of the ZrO_2.

List of Figures **Page No**

List of Tables **Page No**

Chapter 1

GENERAL INTRODUCTION

1.1 Introduction

Zirconia (ZrO_2) is very limited interest as a structural or engineering ceramic due to the displacive tetragonal (t) $\rightarrow$ monoclinic (m) phase transformation, which occurs at ~ 950°C on cooling and is accompanied by a shear strain of ~ 0.16 and a volume expansion of ~ 4%. This change of shape in the transforming volume can result in catastrophic fracture and hence, structural unreliability of fabricated components [1]. However, ZrO_2 has other intrinsic physical and chemical properties, including hardness, wear resistance, low coefficient of friction, elastic modulus, chemical inertness, ionic conductivity, electrical properties, low thermal conductivity, and high melting temperature that make it attractive as an engineering and structural material. Increase of its industrial applicability has been brought after the discovery of t $\rightarrow$ m transformation which can be controlled by suitable material processing to become the source of transformation toughening. Transformation toughening of ZrO_2 was first reported in a paper entitled "Ceramic Steel?" by Garvie, Hannink, and Pascoe [2]. This title was purposely chosen to emphasize the features that ZrO_2 ceramics have in common with alloys of iron. ZrO_2 has a thermal expansion coefficient and elastic modulus similar to those of steel. Also, similar to iron, ZrO_2 has several allotropes, and it can be alloyed to achieve a variety of microstructures and resulting properties.

1.2 Different polymorphs of ZrO_2

Bulk ZrO_2 is polymorphic, exhibiting cubic (c) fluorite structure [Zr atoms are coordinated to eight oxygen atoms], tetragonal (t) structure [distorted fluorite structure whose diffraction patterns can be indexed to a face centered tetragonal cell] and monoclinic (m) structure [sometimes referred to as the baddeleyite structure]. The transformation from m-phase to t- or c-phase is reversible so the high temperature polymorphs do not retain on cooling back to room temperature. Pure ZrO_2 has monoclinic structure at room temperature and undergoes m$\rightarrow$ t and t$\rightarrow$ c phase transitions at 1173°C and 2370°C respectively [3, 4].

1.3 Stabilized ZrO_2

It has been found that the high temperature ZrO_2 forms can be stabilized at room temperature by addition of a small amount of oxides as MgO, CaO, Y_2O_3, CeO_2 etc [5, 6]. Stabilization of t or c -ZrO_2 at low temperature is still a matter of controversy. Garvie [7] developed the following equation for critical grain size in pure unconstrained ZrO_2 based on surface free energy considerations as given below.

1.3.1 Influence of particle size

On the basis of the lower value of the surface energy t-phase (γ_t) in relation to m-phase (γ_m), Garvie [7] considers that in order to stabilize t- phase at low temperature the following equation must be satisfied:

$$(G_t - G_m) + S_t\gamma_t - S_m\gamma_m \leq 0$$

Where G is the molar free energy and S is the surface area in the single crystal particle. It was determined that particle size for stabilizing t- phase must be ≤ 30 nm.

1.3.2 Stabilization by lattice strain

It is suggested that domain boundaries inhibit t → m transition; existence of an active nucleation site and mobility of grain boundaries can be strongly reduced by pores, dopants and particles of a second phase. The most stable polymorphic phase is the one that has the lowest free energy under given conditions (composition, temperature and pressure).

1.4 Chemistry of ZrO_2

Zr and Hf have a chemical behavior and bonding characters, which are dramatically different from other metallic elements. This could be one of the main reasons that ZrO_2 is different in many ways from other metal oxides. Most investigators have treated ZrO_2 just as other metal oxides in the assumption that ZrO_2 is a pure ionic crystalline compound. This is not quite correct. From its location in the periodic Table, the characteristic valence of Zr should be 4, and its maximum coordination number should be 8. However, in reality, it appears that Zr hardly ever forms a monoclinic ion (Zr^{4+}) in its compounds at ambient temperature.

Zr atoms do not give up electrons so that they never exhibited a net positive charge but they do accept electrons and could exhibit net negative charges. It is suggested that Zr atom is not large enough for ionization with a quadruple charge. When approximately 50% of Zr^{4+} ion becomes seven coordinated, a stable single cubic phase or a fully stabilized ZrO_2 can be obtained. This is with about 5to 6 % vacancies in cations, such as $Ca^{2+}$and Y^{3+}, entering the structure are still at a minimal level, and the anion vacancies (5 - 6%) is probably sufficient for the O^{-2} ions to move at a minimum activation energy. Therefore, these compositions always show maximum conductivity. In contrast, the entrance of more large cations into the structure not only slows down more Zr^{4+} ions to become seven coordinated, but the structure is therefore more stable and more covalent and less conductive.

1.5 Application of ZrO_2

High melting point and excellent chemical properties of ZrO_2 makes it useful as an excellent refractory material, abrasive resistance, surface coating, structural components, catalyst and catalyst support [8-9]. Small components of ZrO_2 and its ceramic composites are common in automobiles and other applications. Being a toughened ceramic material it is used as slide gate valves, cutting tools, bowls, and hard grinding balls. Stabilized c-ZrO_2 has special applications as oxygen sensors, determination of pollutant gases and high temperature solid oxide fuel cells (SOFC) [10-*13*]. The SOFC applications have recently been attracting more worldwide attention, due to their high energy transfer efficient and environment concerns.

1.6 Organization of project report

The physical size of ZrO_2 when reduced to nano dimensions, it affects the structure and phase transformation behavior. Preliminary introduction about ZrO_2 with different polymorphs, stabilization, chemistry, application of ZrO_2 and organization of project report is discussed in chapter 1. Chapter 2 provides a detailed discussion of literature on the effect of pH, size and temperature on polymorphs of ZrO_2 without any stabilizer. The main objective of the present work, which is based on the literature survey, is presented towards the end of chapter 2. In chapter 3, the various synthesis and characterization techniques used in the present work are described in detail. Chapter 4 describes the synthesis and characterization of ZrO_2 prepared through geletion and precipitation using $NaBH_4$, NH_4OH and N_2H_5OH. Finally, conclusions of this project work are given in Chapter 5.

Chapter 2

LITERATURE REVIEW

2.1 Effect of pH, size and temperature on polymorphs of ZrO_2 without any stabilizer

Interest in nanocrystalline zirconia (ZrO_2) ceramics that have an average grain size < 100 nm has increased during recent years due to their unusual properties such as sintering ability, mechanical toughness, and superplastic behavior [14]. There are different routes (such as chemical precipitation, hydrothermal, gas-condensation, sonochemical, and sol–gel processes) are developed to synthesize stabilized *t*- or *c*-ZrO_2 in well-defined particle size or morphology [15-19]. The stabilization of the t- phase at low temperatures is due to the lower surface free energy of this phase. It was calculated that if the critical particle size limit of 30 nm is exceeded, the tetragonal particles are transformed to the monoclinic phase [20]. Many investigators have verified this concept by stabilizing t or c phase of ZrO_2 at low temperature with as well as without stabilizer. There are very few reports which are discussed as below on the synthesis of *t*- or *c*-ZrO_2 in small crystallites without any stabilizer by varying pH, size and temperature.

Osendi et. al. [21] have studied the two kinds of ZrO_2 powders by: (a) precipitation with ammonia (pH = 10) from a zirconium oxychloride and (b) thermal decomposition of zirconyl acetate. It has been observed that the starting transformation of t-m ZrO_2 was at 700 °C and completed at 1100 °C for sample prepared though ammonia. However, this transformation occurred suddenly at ~ 950 °C for sample prepared though thermal decomposition. It indicates that the formation of lattice defects by the evolution of impurities during crystallization can be associated with the nucleation of the tetragonal phase. In both the cases, when the average size of the tetragonal crystallites reaches values close to the critical crystallite size determine by Garvie [7] (≈ 30 nm), the monoclinic phase observed.

Srinivasan et. al. [22] have studied the crystallite size effect on the low-temperature transformation of t-phase ZrO_2. It was synthesized by precipitation from a solution of $ZrCl_4$ by adding NH_4OH to produce a pH of 2.95. The as-prepared powders were calcined at 500 °C for periods ranging from 15 to 200 h. The major fraction of t-phase formed at 15h calcination and a large fraction was transformed to the m-phase after 200 h of heating at 500 °C.

Igawa et. al. [23] have studied the crystal structure of metastable tetragonal zirconia prepared by alkoxide method without any dopant has been examined by nutron diffraction at room temperature. The precursor was formed by the reaction of tetra-n-butoxide [$Zr(^nOC_4H_9)_4$] with C_2H_5OH. The t-phase of ZrO_2 (crystallite size ~ 16 nm from XRD and mean particle size ~ 5μm from SEM) was formed when the as-prepared powders were heat-treated at 700 °C for 15 minutes in air and then quenched to room temperature. When the as-prepared powders were heat-treated at 1200 °C, it clarifies the similarity between this

metastable phase and the tetragonal phase at high temperature using neutron diffraction [24]. The lattice constant, tetragonality, oxygen shift parameters and equivalent isotropic thermal parameter of the metastable tetragonal phase are proportional to the temperature. These parameters, when extrapolated to the high-temperature range, are very similar to those of the high temperature tetragonal phase. This paper indicated that the structure of the metastable tetragonal phase is the same as that of the high temperature tetragonal phase.

Bandyopadhyay et. al. [25] have synthesized microcrystalline ZrO_2 in monoclinic form on the gold foil at room temperature via electrochemical technique. Almost epitaxial growth was observed with crystal sizes in the range of 5 – 15 μm. This thin film of ZrO_2 on the metal surface will be interesting for fundamental as well as technical applications such as catalysis and oxygen sensors. In addition, this process could possibly be extended to stabilize t-ZrO_2 / c-ZrO_2 at room temperature by controlling the electrolyte composition and the condition of the electrochemical techniques.

Berry et. al. [26] have synthesized ZrO_2 by hydrothermal process using zirconium (IV) acetate as a precursor. The pH was maintained by adding HCl (pH- 1) and NH_4OH (pH- 10). At high pH of the precursor prepared through NH_4OH shows mixture of t- and m- phase of ZrO_2 when heat-treated at 500°C. As the temperature increases t-phase decreases and m-phase increases. At 900 °C, the t- and m-phase of ZrO_2 is in the ratio of 43:57 respectively. In case of HCl treatment, the high temperature treated (500 °C onwards) powders contains only m-phase of ZrO_2. In this paper, effect of pH is studied on the formation of ZrO_2 from zirconium acetate solution. Zirconia formed from solution of high pH was found to contain greater quantity of tetragonal polymorphs, suggesting that the addition of alkali to the solution leads to stabilize the tetragonal form against conversion to the monoclinic form.

Xia et. al. [27] have synthesized ZrO_2 nanopowders prepared by low temperature vapor-phase hydrolysis of inorganic $ZrCl_4$. It has been reported that the ZrO_2 nanopowders was characterized by small size (5.8 nm), narrow size distribution, near spherical shape and having high surface area (150 m^2/g) with weak agglomeration. Both t- (91%) and m- (9%) phase of ZrO_2 have been observed in this route when the as-prepared powders were heat-treated at 500 °C. The m-phase content increases with elevated calcination temperature, while t-content decreases.

Wu et. al. [28] have synthesized tetragonal ZrO_2 nanocrystallites with or without yittria (3 mol %) doping using precipitation process in which hydrous oxide precipitate reacts with hexamethyldisilazane (HMDS) vapour before calcination. The tetragonal structure retained for hours after calcination at temperatures of 300 °C – 1100 °C. The enhanced structural

metastability has been attributed to the combined effect of suppressed grain growth and reduced surface energy that results from the HMDS treatment.

Mondal et. al. [29] have synthesized monolithic t-ZrO_2 nanopowders with an amorphous $ZrO(OH)_2.xH_2O$ polymer precursor by using NH_4OH. The final pH of the precursor solution was nearly 10. It has been observed that the polymer precursor solution has thermal decomposition in self stabilized t-ZtO_2 nanoparticles (size ~ 8nm) at temperature as low as 200 °C. The particles grow no larger than 12 nm at 600 °C with the presence of 10 % m-phase and 90 % t-phase of ZrO_2. Pure m-ZrO_2 appears with a sudden growth of size 22 nm at as low a temperature as 800 °C. Qualitatively, a high level of oxygen vacancies and manifested grain surface seem to determine the metastable t-ZrO_2 structure in small crystallites.

Lee et. al. [30] have synthesized amorphous hydrous ZrO_2 nanoparticles by using water in supercritical carbon dioxide by adding an aqueous ammonia solution. This synthesis proves to be an effective method for making nanoparticles because of the ability to manipulate the pressure and temperature to control the particle size and morphology. As the precursor reaction was increased from 13.9 to 17.3 MPa, the size of the ZrO_2 particles was decreases from 60nm to 10nm, with the change in morphology. The t-phase of ZrO_2 is observed at low temperature of 450 °C and it coverts to m-phase from 550 °C onwards.

2.2 Summary of Literature

Summary of the literature survey are:

(1) There are different routes as discussed in the literature part for stabilization of t-ZrO_2 without any stabilizer.

(2) Most work had done by hydrolyzing the Zr-salt by using either NH_4OH or C_2H_5OH or HCl.

(3) Different polymorphs of ZrO_2 are dependent on pH, crystallite size and calcination temperature.

(4) High pH of the initial precursor solution has better stability on t-ZrO_2 as compared to low pH at elevated temperature.

(5) Development of the monoclinic phase is observed when the tetragonal crystallite of ZrO_2 reaches values close to that of critical crystallite size (~ 30nm).

(6) As the temperature increases, the crystallite size increases and simultaneously t-phase of ZrO_2 decreases.

(7) Stabilization of metastable t-ZrO_2 in most cases is up to 500 °C without any stabilizer.

2.3 Objective of the present studies

Few works have been reported on stabilization of t-ZrO_2 without any stabilizer by hydrolysis of Zr-salt using NH_4OH by precipitation and hydrothermal technique. But no such study had been done for stabilizing the t-phase without any stabilizer by reduction method. Most of the works have been done at high pH of the initial precursor solution while very few works has reported on low pH. No such literatures are found on stabilization of t- ZrO_2 by both geletion and precipitation technique using a reducing agent. The main objectives of the present study are:

(1) Synthesis of ZrO_2 polymorphs using both reduction and hydrolysis technique.

(2) These techniques are known to result in the production of nanocrystalline materials. Also, promote the stabilization of metastable t-ZrO_2 at the nano level at moderate temperature, which is one of the primary objective of this work.

(3) Enhancement of metastable t- ZrO_2 through geletion (low pH) and precipitation (high pH) route by using sodium borohydride, $NaBH_4$ (a strong reducing agent) and hydrazine hydrate, N_2H_5OH (a weak reducing agent) and NH_4OH (a hydrolyzing agent).

(4) Study and compare the thermal, structural, microstructural, and IR results of the as-prepared as well as calcined ZrO_2 powders.

Chapter 3

EXPERIMENTAL WORK

3.1 Introduction

Sol-gel and precipitation technique is one of the important techniques for synthesizing nanosize ceramic materials. In this work, nano size ZrO_2 has been prepared through gelation and precipitation techniques. Several different characterization techniques have been used to study the properties of nano ZrO_2 powders. In this chapter, the synthesis and characterization techniques are described in detail.

3.2 Synthesis

Nanosize zirconia powders were prepared through gelation and precipitation technique by using $NaBH_4$ (Sodium Borohydride), NH_4OH (Ammonium Hydroxide) and N_2H_5OH (Hydrazine Hydrate). An aqueous solution of 0.5 *M* (where *M* is the molarity) concentration of $ZrOCl_2.8H_2O$ were prepared from high purity salt. The Zr-salt solution is highly acidic with a pH of ~ 0.3. On the other hand the $NaBH_4$, NH_4OH and N_2H_5OH solution has a highly basic pH of ~ 10. This solution is added drop wise to the Zr-salt solution so that gel formation will take place at a particular pH depending on the reducing or hydrolyzing agents. The reaction mechanisms for all these cases can be expressed as follows.

3.2.1 Reduction by $NaBH_4$

The formation and evolution of nanosize zirconia powders is studied as a function of reaction with Zr-salt solution by $NaBH_4$. As $NaBH_4$ is highly reducing agent, the exothermic reaction occurs in successive steps depending on the initial concentration of precursor solutions, the local temperature during the reaction, and other experimental conditions. The reaction in a simple form for all three cases can be expressed as follows

$$4\ ZrOCl_2.8H_2O + 2\ NaBH_4 \rightarrow\ 2\ ZrCl_3 + 2\ Zr(OH)_4 + 25\ H_2O + 2\ NaCl + B_2O_3 + 7\ H_2\uparrow \quad (3.1)$$

$$ZrCl_3 + 4\ OH^- + 3\ Na^+ \rightarrow\ Zr(OH)_4 + 3\ NaCl \quad (3.2)$$

$$Zr(OH)_4 + H_2O \rightarrow ZrO(OH)_2 + 2\ H_2O \quad (3.3)$$

The exact reduction reaction of $ZrOCl_2$ in presence of $NaBH_4$ is not clearly known but the plausible mechanisms are; (i) Zr-gel formation releases nascent hydrogen which leads to better reduction of Zr^{+4} to Zr^{+3} cations (ii) formation of transient lower oxidation state of Zr, (iii) Simultaneously Zr^{+3} state will convert to Zr^{+4} in the form of $Zr(OH)_4$ as due to the unstable behavior of $ZrCl_3$ and (iv) Finally $Zr(OH)_4$ is hydrolyzed to $ZrO(OH)_2.2H_2O$ which indicates gel formation.

3.2.2 Reduction by N_2H_5OH

The formation and evolution of nano size zirconia powders is studied as a function of reaction with Zr-salt solution by N_2H_5OH. The process involves a controlled hydrolysis of Zr^{+4} cations to $ZrO(OH)_2$ in this cases.

$$ZrOCl_2 + 2N_2H_5OH \rightarrow ZrO(OH)_2 + 2NH_4Cl + N_2 \uparrow + H_2 \uparrow \quad (3.4)$$

3.2.3 Hydrolysis by NH_4OH

The evolution of nano size zirconia powders is studied as a function of reaction with Zr-salt solution by both NH_4OH. The process involves a controlled hydrolysis of Zr^{+4} cations to $ZrO(OH)_2$ in this case.

$$ZrOCl_2 + 2NH_4OH \rightarrow ZrO(OH)_2 + 2NH_4Cl \quad (3.5)$$

The reaction occurred slowly and there was a regular increase of average viscosity of the solution. It has been observed that gel formation was formed at low pH of nearly 3.0, 4.4 and 4.0 for $NaBH_4$, NH_4OH and N_2H_5OH respectively. After the gel formation, the precursor solution was increases to high pH of ~ 8.7 so that complete precipitation will take place for all these three cases by adding more amounts of reducing and hydrolyzing agents. Low pH as well as high pH of all precursor solution was allowed progress for nearly 5 days durations of time for complete of reaction before it was extracted for centrifuge. The low as well as high pH precursor was thoroughly washed with distilled water by repeated centrifuging (10,000 rpm) in order to remove the water soluble reaction products completely. The centrifuged products were dried in oven at 80 °C for 24 hrs. The dried powders were grounded in a mortar pestle to form fine powders of as-prepared zirconia. The fine powders (both low as well as high pH) obtained after drying were heat treated at selected temperatures in the range of 500 °C to 1000 °C range for 1 hour to study the formation and thermal stability of ZrO_2 polymorph and also its phase transformation to equilibrium m-ZrO_2 structure. The flow chart used for the preparation of nano size zirconia powders is shown in Fig. 3.1.

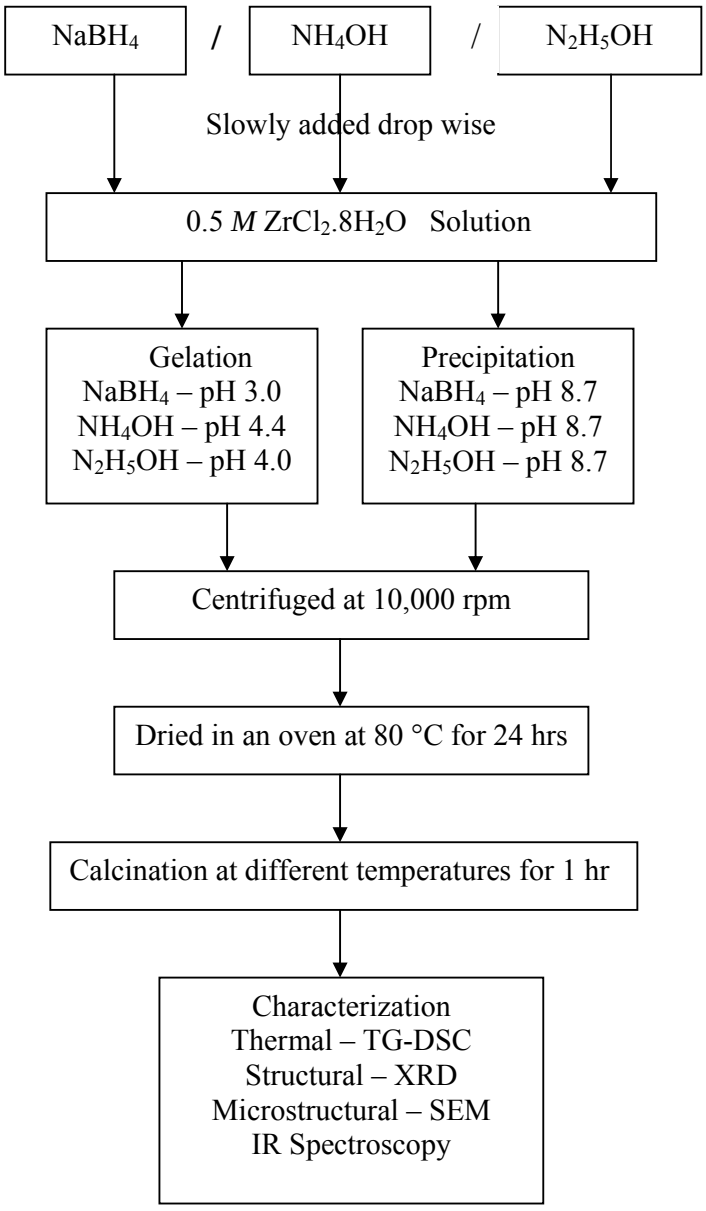

Fig. 3.1: Schematic flow chart for preparation of nano size ZrO_2 powders

3.3 General characterization

3.3.1 Thermal

Thermal decomposition of $ZrO(OH)_2$ gel to an amorphous ZrO_2 powder followed by its reconstructive nucleation of t-ZrO_2 nanoparticles were studied using thermogravimetric and differential scanning calorimetric (TG-DSC) by heating the sample at 10 °C/min in argon in a thermal analyzer (Model STA 4096, NETZSCH , Germany)

3.3.2 X-ray diffraction

Phase analysis was studied using the room temperature powder X-ray diffraction (Model: PW 1830 diffractometer, Phillips, Netherland) with filtered 0.154056 nm Cu Kα radiation. Samples are scanned in a continuous mode from 25° – 90° with a scanning rate of 0.02 (degree) / 1 (sec).

3.3.3 Scanning Electron Microscope

Microstructural features were studied using Scanning Electron Microscope (JSM 6480 LV JEOL, Japan). For preparation of SEM sample, the powder is dispersed in isopropyl alcohol in an ultra sonication bath (20 kHz, 500 W) for half an hour. One drop of the well-dispersed sample solution is deposited on to polished brass plate. This brass plate was used for microscopy.

3.3.4 Particle size measurement

Size of the particles is usually obtained with the help of scanning electron microscopy (SEM). The size corresponds to the mean value of the crystalline domain size of the particles is determined from the X-ray line broadening using Debye-Scherrer formula with correction factor as given below,

$$D_x = \frac{0.9\lambda}{\beta \cos\theta} \quad \text{Where } \beta = \sqrt{\beta^2_{sample} - \beta^2_{standard}}$$

Where D_X is average crystalline size, λ is the X-ray wavelength used, β the angular line width of half maximum intensity and θ the Bragg's angle in degree. Standard value of β is taken as the angular line width of half maximum intensity for polycrystalline SiO_2 material.

3.4.5 IR-Spectroscopy

IR spectra of the powders in KBr pellets were studied in the range of 400 – 4000 cm^{-1} by using IR-spectrometer.

Chapter 4

RESULTS AND DISCUSSION

4.1 Introduction

This chapter describes the thermal, structure, microstructure and Infra-Red analysis of ZrO_2 nanoparticles prepared through gelation and precipitation by reduction and hydrolysis technique using $NaBH_4$, NH_4OH and N_2H_5OH.

4.2 Thermal behavior of as-prepared ZrO_2

Fig. 4.1, 4.2 and 4.3 shows the Thermal Gravimetric (TG) – Differential Scanning Calorimetric (DSC) of as-prepared ZrO_2 powders of two different pHs (geletion at low pH, and precipitation at high pH) prepared from the reaction of $ZrOCl_2.8H_2O$ with $NaBH_4$, NH_4OH and N_2H_5OH respectively.

Fig. 4.1 (a) and (b) shows the TG-DSC curve of pH 3.0 and pH 8.7 respectively of as-prepared zirconia powders prepared from the reaction of $ZrOCl_2.8H_2O$ with $NaBH_4$.

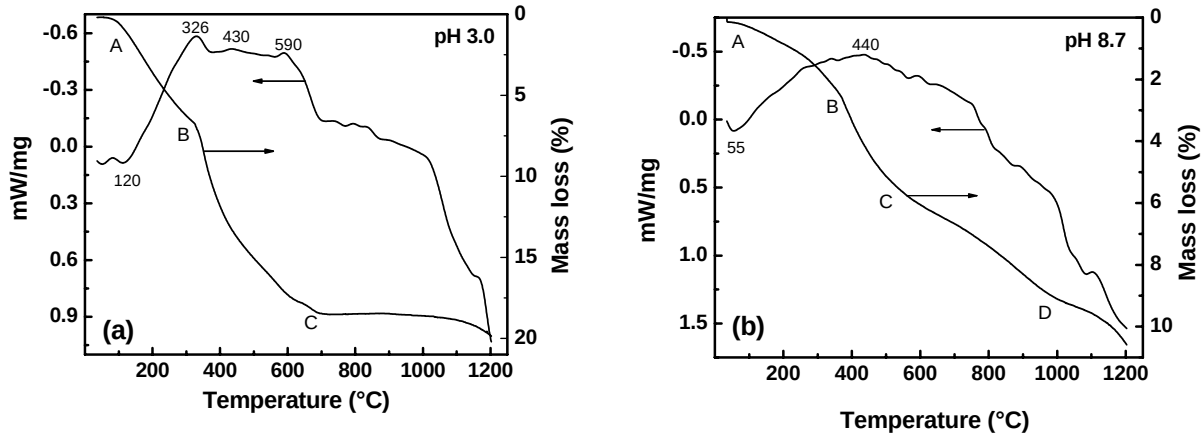

Fig. 4.1 (a) and (b): TG-DSC of pH 3.0 and 8.7 respectively of as-prepared zirconia powders prepared from $NaBH_4$

At low pH 3.0 (Fig 4.1 a), the TG curve shows two stages of major weight loss. One stage ranges from room temperature to 300 °C (region AB in TG curve). In the DSC plot there is an endothermic peak at 120 °C and three exothermic peaks at 326 °C, 430 °C and 590 °C. The TG curve shows that major weight losses (region AB and BC is about 6 % and 12 % weight loss respectively) were associated with both endothermic and exothermic effects. The first exothermic peak at 326 °C may be associated with the decomposition of amorphous hydrous as-prepared zirconia or of trapped solute or solvent during reaction of $ZrOCl_2.8H_2O$ with $NaBH_4$. In addition to this peak, another two weak exothermic peaks is indicated at 430 °C and 590 °C, probably due to crystallization of tetragonal zirconia (t-ZrO_2) by the important weight loss (~ 12 %) is observed. However, it is different case for high pH (8.7) as-

prepared zirconia powders (Fig 4.1 b). There is no apparent exothermic peak; with a small amount of weight loss (about 4 % in the region BC in TG curve of Fig. 4.1 b) is observed. High pH (~ 8.7) TG-DSC patterns are greatly different from those of low pH (3.0) may be due to the particle size effect or the powders contains oxides other than hydrates. At low pH there is no significant weight loss after 675 °C where as at high pH; there is continuous weight loss up to 1200 °C.

Fig. 4.2 (a) and (b) shows the TG-DSC of pH 4.4 and pH 8.7 respectively of as-prepared zirconia powders prepared from the reaction of $ZrOCl_2.8H_2O$ with NH_4OH.

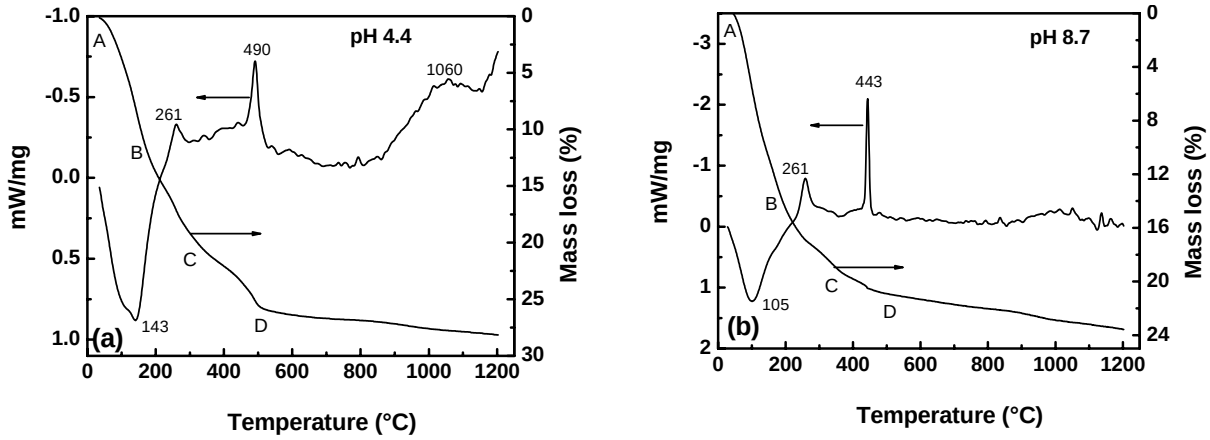

Fig. 4.2 (a) and (b): TG-DSC of pH 4.4 and 8.7 respectively of as-prepared zirconia powders prepared from NH_4OH

The TG-DSC curves look similar for both low as well as high pH powders. There is an endothermic peak in the range of 50 °C – 180 °C for both pHs corresponds to ~ 12 % weight decrease over this temperature range. This is due to desorption of absorbed water on the surface of ZrO_2 powders. The total mass loss is about ~ 28 % for low pH and about ~ 23 % for high pH upto 1200 °C. Two exothermic peaks are observed for both pH powders. First exothermic peak at 261 °C indicates the decomposition of amorphous hydrous zirconia precursor or of trapped solute or solvent during reaction of $ZrOCl_2.8H_2O$ with NH_4OH. At low pH the crystallization temperature of t-phase of ZrO_2 is observed at 490 °C with a weight loss ~ 5 % in the region CD of Fig. 4.2. (a). However; at high pH, the crystallization temperature decreases to 443 °C with a weight loss of ~ 2 % in region CD of Fig. 4.2 (b). The decrease of crystallization temperature of t-ZrO_2 may be due to particle size effect.

Fig. 4.3 (a) and (b) shows the TG-DSC of pH 4.0 and pH 8.7 respectively of as-prepared zirconia powders prepared from the reaction of $ZrOCl_2.8H_2O$ with N_2H_5OH.

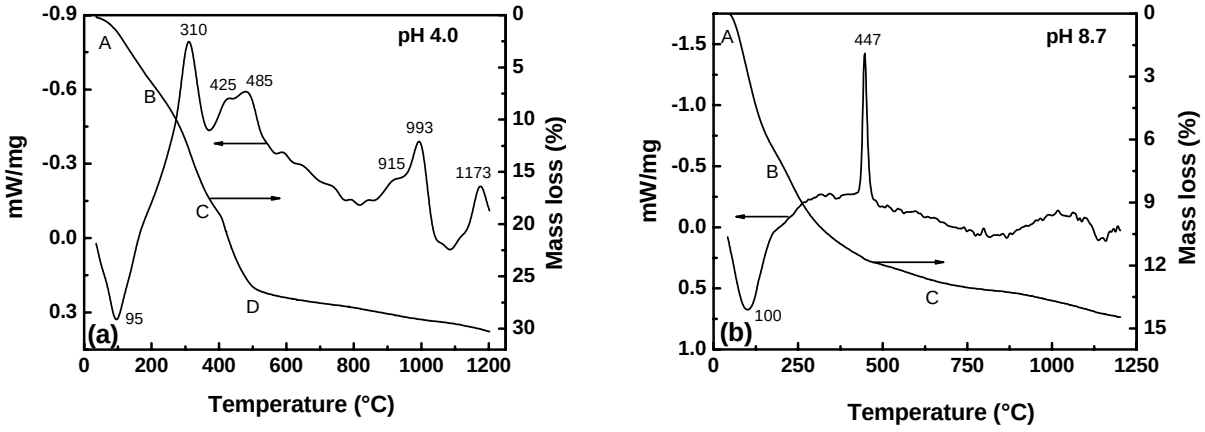

Fig. 4.3 (a) and (b): TG-DSC of pH 4.0 and 8.7 respectively of as-prepared zirconia powders prepared from N_2H_5OH

There is an endothermic peak at ~ 100 °C in DSC curve for both low pH as well as high pH zirconia precursor powders prepared from hydrazine hydrate (N_2H_5OH). This endothermic peak indicates the removal of water molecule from the surface of zirconia powders with a significant weight loss around 7 % in both cases. The total mass loss is about ~ 30 % for low pH and about ~ 15 % for high pH upto 1200 °C. At high pH, the crystallization temperature of t- ZrO_2 is clearly seen at around 447 °C with a weight loss of around 5 % in the region BC in Fig. 4.3. (b). However, there is no sharp crystallization temperature of t-ZrO_2 is observed in the case of low pH powders (Fig. 4.3. a). There are three exothermic peaks at 310 °C, 425 °C and 485 °C for low pH powders. The first exothermic peak at 310 °C may be associated with the decomposition of amorphous hydrous zirconia precursor or of trapped solute or solvent during reaction of $ZrOCl_2.8H_2O$ with hydrazine hydrate. In the low pH powders, the crystallization temperature of t-ZrO_2 is in the range of 425 °C – 485 °C. At higher temperature (915 °C, 993 °C) two additional exothermic effects are also present.

From the TG-DSC curve, it has been clearly observed that the crystallization temperature of t-ZrO_2 is nearly 445 °C for high pH (8.7) zirconia powders in all cases except for $NaBH_4$. However, for low pH powders, a broad and high crystallization temperature of t-ZrO_2 is observed. Also weight loss of low pH powders is higher than the high pH. This effect may be due to the particle size of ZrO_2 powders.

4.3 Structure and microstructure

The presence of various phases and crystallite size were determined from the X-ray diffraction pattern. Fig. 4.4 shows the X-ray diffraction pattern of the dried as-prepared ZrO_2 powders before washing with distilled water. It has been observed that NaCl is present in the as-prepared powder when Zr-salt is reacted with $NaBH_4$. However no peaks are observed when Zr-salt is reacted with N_2H_5OH and NH_4OH. As per the reaction equation (described in chapter 3), the Cl^- ions are present in case of both N_2H_5OH and NH_4OH process. These are not clearly visible from the XRD pattern. Hence, the as-prepared powders are washed and centrifuged for several times (~10 times) with distilled water to remove the Cl^- ions, NaCl salt as well as borate phase.

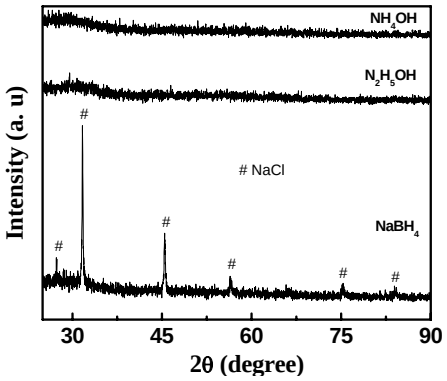

Fig. 4.4: X-ray diffraction patterns of ZrO_2 powders before washing with distilled water

The washed and dried powders are heat-treated at elevated temperatures so that different polymorphs of ZrO_2 are formed at different temperatures. Figs. 4.5 (a), (b) (c) and (d) show the XRD pattern of ZrO_2 powders calcined at 500 °C, 600 °C, 700 °C, and 800 °C for 1 hour respectively for two different pHs prepared from $NaBH_4$. It has been seen that tetragonal zirconia (t-ZrO_2) is developed at 500 °C (Fig. 4.5 a) for both low as well as high pH powders. All the peaks are assigned to t- ZrO_2 in a single crystalline phase as marked by (hkl) values. An average crystallite size of t-ZrO_2 is found to be 7 nm by using Debye Scherrer relation. As the temperature increases, the crystallinity of low pH powders is found to be more compared to high pH powders. Tetragonal ZrO_2 stability is observed upto 600 °C for both pHs powders (Fig. 4.5 b). A further increase in temperature leads to growth of crystallite size for both pHs but the t-ZrO_2 stability is more at low pH compared to high pH powders. An activated grain growth operates in fully monoclinic zirconia (m-ZrO_2) if the temperature is increased above 800 °C. The crystallite size and phase composition of ZrO_2 powders prepared through $NaBH_4$ is given in Table 4.1.

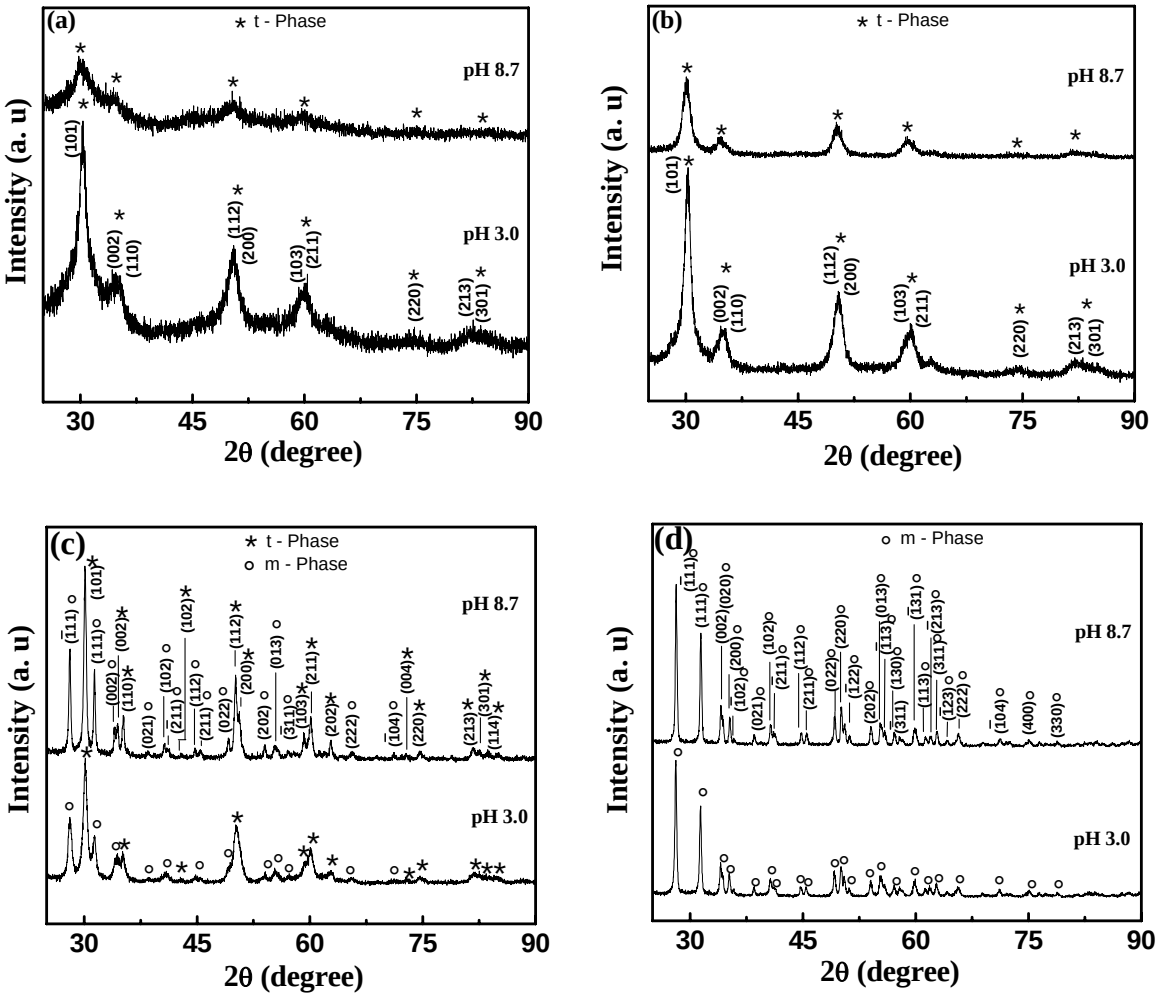

Fig. 4.5: X-ray diffraction patterns of ZrO_2 powders (synthesized from $NaBH_4$) calcined at (a) 500 °C, (b) 600 °C, (c) 700 °C and (d) 800 °C for 1 hour

Table 4.1: Crystallite size and phase composition of ZrO_2 (synthesized from $NaBH_4$)

Sample	Temperature (°C)	Crystallite Size	t – Phase	m - Phase
pH 3.0	RT		Amorphous	
	500	7	100	0
	600	8	100	0
	700	15	57	43
	800	30	0	100
pH 8.7	RT		Amorphous	
	500	4	100	0
	600	7	100	0
	700	23	50	50
	800	29	0	100

Figs. 4.6 (a), (b), (c), (d), and (e) show the XRD pattern of ZrO_2 powders calcined at 500 °C, 600 °C, 700 °C, 800 °C and 850 °C for 1 hour respectively for two different pHs prepared from NH_4OH.

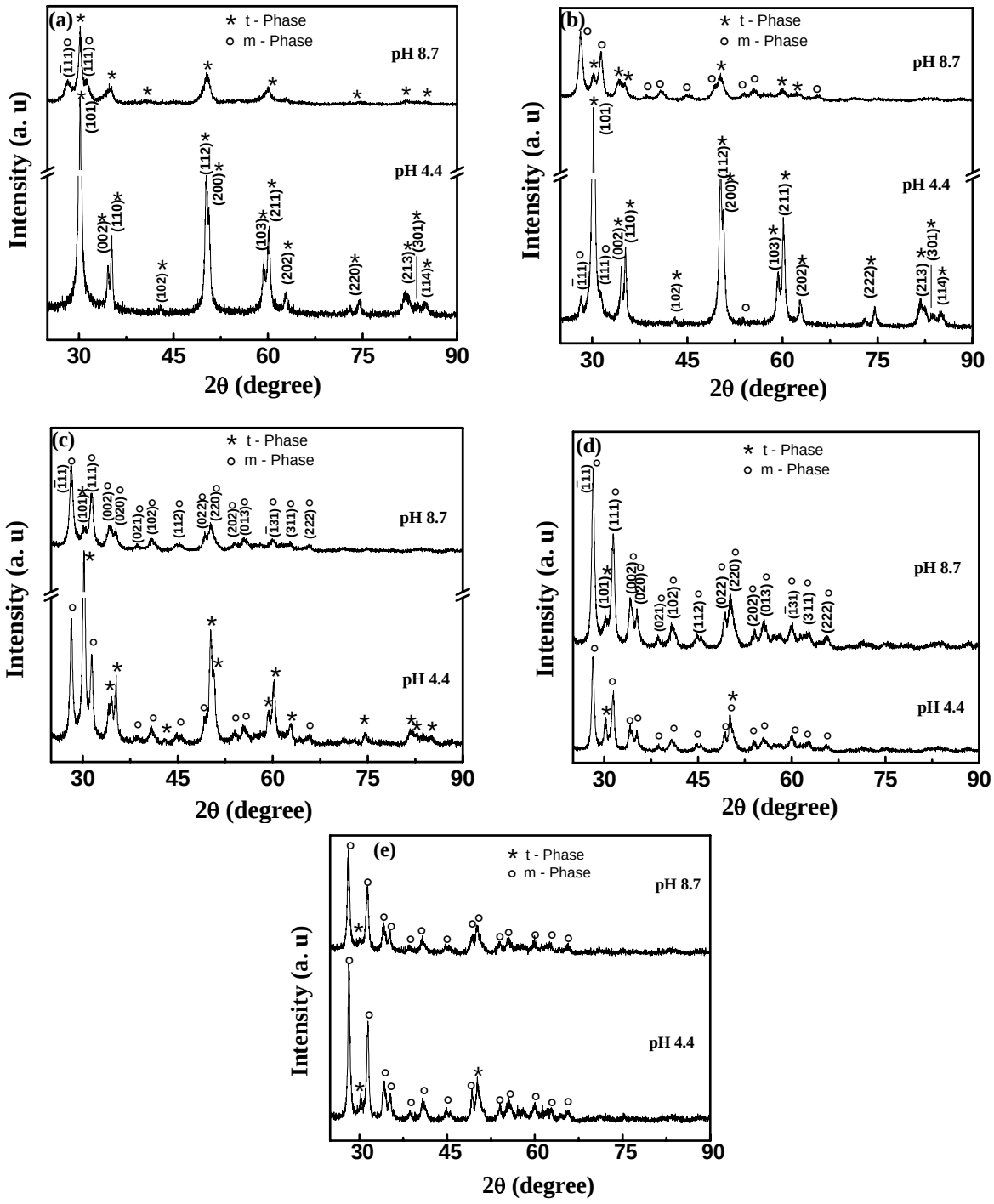

Fig. 4.6: X-ray diffraction patterns of ZrO_2 powders (synthesized from NH_4OH) calcined at (a) 500 °C, (b) 600 °C, (c) 700 °C (d) 800 °C and (e) 850 °C for 1 hour

It has been observed that only t-ZrO_2 is developed for low pH powders, whereas mixture of t- (71 %) and m- (29%) ZrO_2 for high pH powders calcined at 500 °C. As calcination temperature increases, the t ZrO_2 decreases at a faster rate for both pH powders. There is sudden increase of m-ZrO_2 as the temperature increases from 500 °C to 600 °C for high pH powder. Small amount of t-ZrO_2 (< 5 %) is still observed up to 850 °C for both pH powders. The crystallite size and phase composition of ZrO_2 powders prepared through NH_4OH is given in Table 4.2.

Table 4.2: Crystallite size and phase composition of ZrO_2 (synthesized from NH_4OH)

Sample	Temperature (°C)	Crystallite Size	t – Phase	m - Phase
pH 4.4	RT		Amorphous	
	500	23	100	0
	600	24	95	5
	700	24	60	40
	800	24	15	85
	850	26	5	95
pH 8.7	RT		Amorphous	
	500	19	71	29
	600	18	19	81
	700	27	8	92
	800	32	5	95
	850	32	2	98

Figs. 4.7 (a), (b) (c) and (d) show the XRD pattern of ZrO_2 powders calcined at 500 °C, 600 °C, 700 °C and 800 °C for 1 hour respectively for two different pHs prepared from N_2H_5OH. The phase formation of ZrO_2 polymorphs through hydrazine hydrate (N_2H_5OH) process is similar to ammonium hydroxide (NH_4OH) process. But the decrease of t-ZrO_2 is very slower rate as compared to NH_4OH process for low pH powders from 500 °C onwards. For low pH powders, the t-ZrO_2 (~ 5 %) is still observed upto high temperature of 950 °C (see Fig. 4.8). However, fully m-ZrO_2 is observed for high pH powders from 850 °C onwards. The crystallite size and phase composition of ZrO_2 powders prepared through N_2H_5OH is given in Table 4.3.

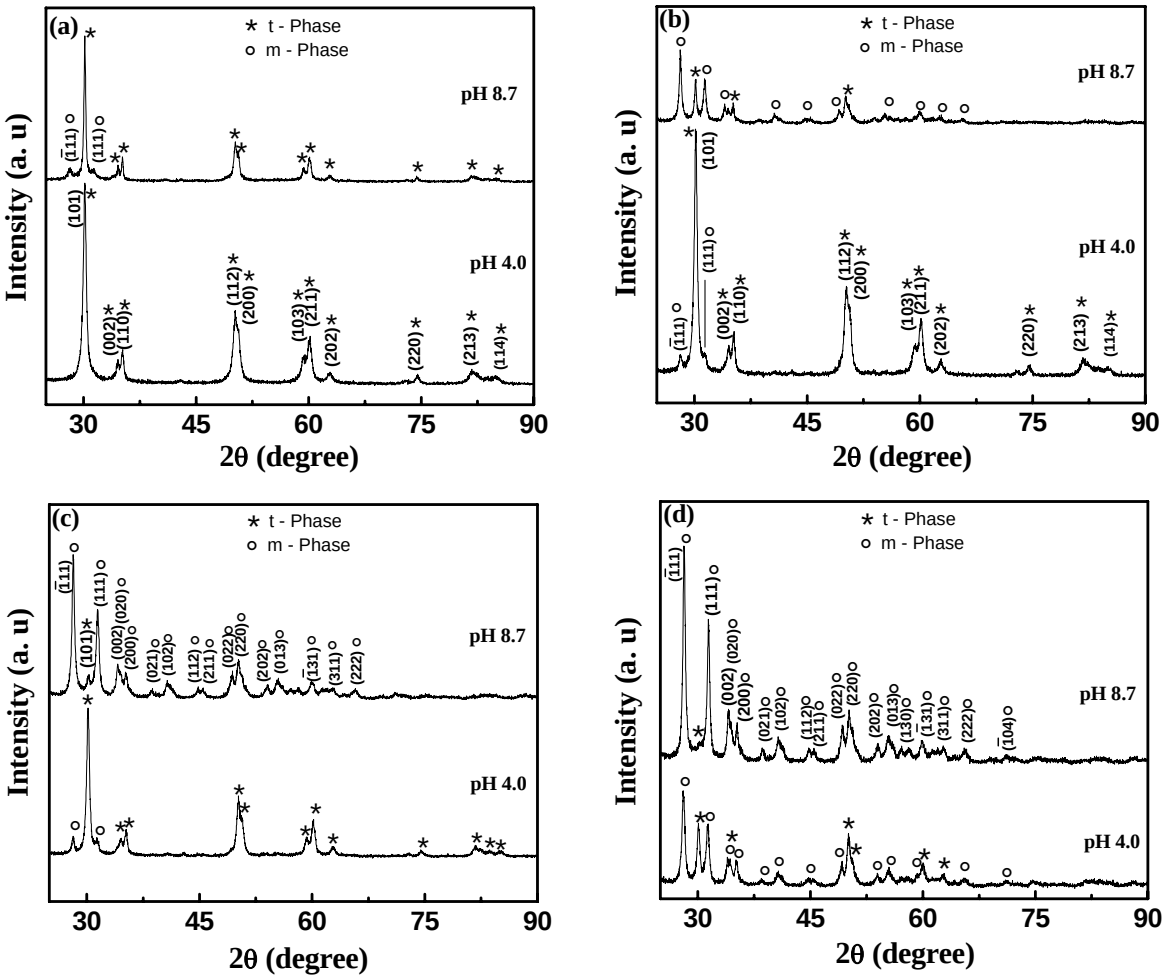

Fig. 4.7: X-ray diffraction patterns of ZrO_2 powders (synthesized from N_2H_5OH) calcined at (a) 500 °C, (b) 600 °C, (c) 700 °C and (d) 800 °C for 1 hour

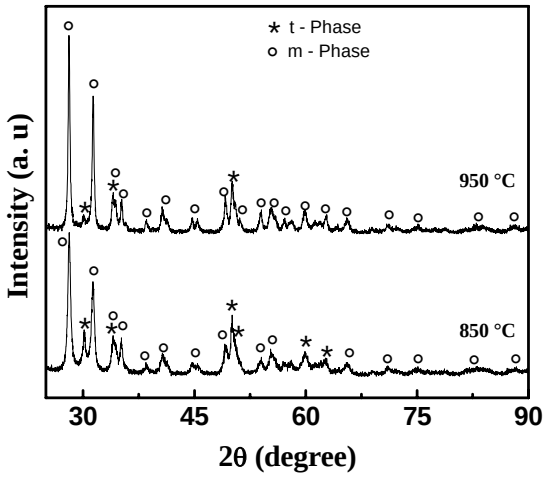

Fig. 4.8: X-ray diffraction patterns of low pH (4.0) ZrO_2 powders synthesized from hydrazine hydrate and calcined at 850 °C and 950 °C.

Table 4.3: Crystallite size and phase composition of ZrO_2 (synthesized from N_2H_5OH)

Sample	Temperature (°C)	Crystallite Size	t – Phase	m - Phase
pH 4.0	RT		Amorphous	
	500	17	100	0
	600	18	92	8
	700	19	86	14
	800	21	29	71
	850	26	13	87
	950	24	2	98
pH 8.7	RT		Amorphous	
	500	28	91	9
	600	29	27	73
	700	27	6	94
	800	22	1	99

Scanning Electron Microscopy (SEM) gives the information about the size, shape and agglomeration behavior of ZrO_2 powders. Fig. 4.9 (a), (b) and (c) show the microstructural SEM image of low pH calcined (600 °C) ZrO_2 powders synthesized from $NaBH_4$, NH_4OH and N_2H_5OH respectively.

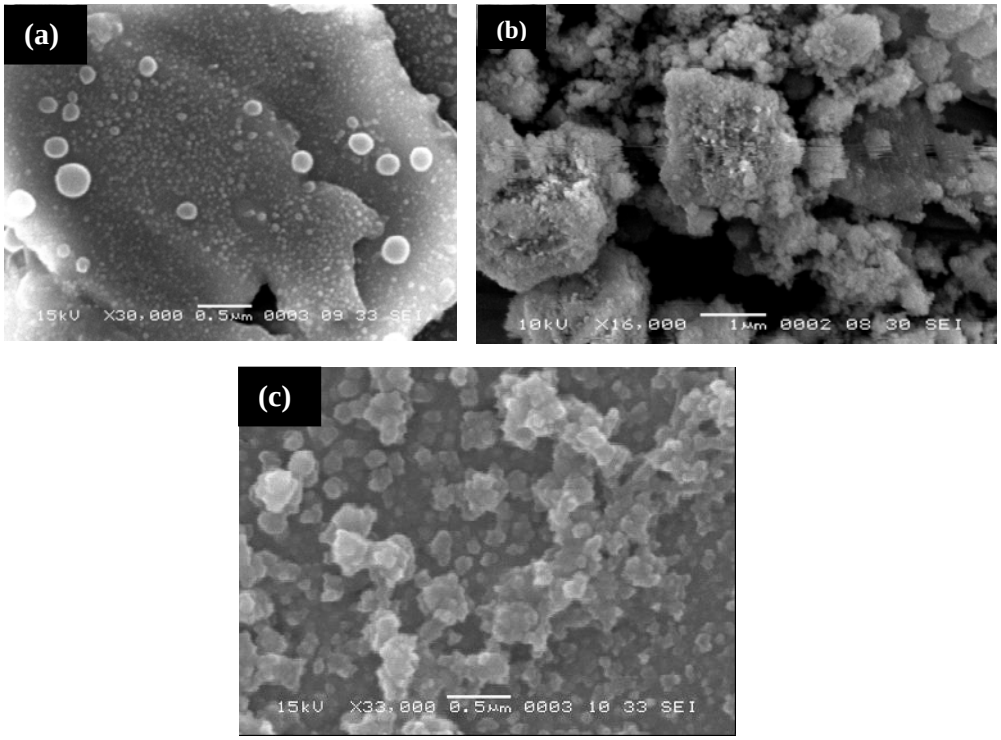

Fig. 4.9: SEM micrographs of low pH calcined (600 °C) ZrO_2 powders synthesized from (a) $NaBH_4$ (b) NH_4OH and (c) N_2H_5OH

The morphology of ZrO_2 synthesized from three routes is different. In case of $NaBH_4$ (Fig.4.9 a), the particle size is nearly spherical in the range of 50 to 200 nm and is non-agglomerate in nature. However, the particle size is nearly spherical and agglomerate in nature for other two routes as seen from the Fig. 4.9 (b) and (c). In all three routes the particle size is in the nanometer range.

4.2.3 IR spectra of as-prepared as well as calcined ZrO_2 powders

Infra-Red spectra in the range of 400 – 4000 cm^{-1} for ZrO_2 powders (as-prepared as well as calcined) synthesized at low pH through $NaBH_4$, NH_4OH and N_2H_5OH is shown in Fig. 4.10, 4.11 and 4.12 respectively. In all cases, $ZrO(OH)_2$ is converted to t-ZrO_2 or m-ZrO_2 derivatives on heating at elevated temperatures. Individual bands of Zr-O group vibrations exist in both $ZrO(OH)_2.xH_2O$ and ZrO_2 derivatives. Also O-H bending and stretching vibrations exist in $ZrO(OH)_2$ and H_2O molecule. The OH group is distinguished easily in the H_2O molecule by its bending vibration which appears in a single band at ~1640 cm^{-1} in water. A strong band is present ~ 1630 cm^{-1} in the as-prepared powder for all cases confirm the presence of water in $ZrO(OH)_2$. Another O-H bending vibrations in the hydroxyl group in the $ZrO(OH)_2$ molecule appears at ~ 1400 cm^{-1} for all as-prepared ZrO_2 powders. As the heating temperature increases, O-H band decreases. One asymmetric O-H stretching band occurs in H_2O in the range of 3350 to 3430 cm^{-1} for all ZrO_2 as-prepared powders. From the IR spectra for all the as-prepared powders reveal that the ZrO_2 nano powders have significant amount of surface-adsorbed H_2O molecules. However ZrO_2 prepared through hydrazine hydrate (N_2H_5OH) shows five bands at 3295, 3237, 3135, 3035 and 950 cm^{-1} are due to the stretching vibrational mode (N-N) of hydrazine hydrate. Furthermore, the spectrum of four distinct bands of *m*-ZrO_2 nanocrystals at around 742, 585, 500, and 415 cm^{-1} differs significantly from the spectrum of the bulk *m*-ZrO_2 in five bands at 730, 588, 520, 445, and 420 cm^{-1}. However no sharp band of Zr-O is observed for t-ZrO_2 in elevated temperatures. The infrared characteristics bands observed in the as-prepared as well as derived t-ZrO_2 and m-ZrO_2 nanopowders prepared through $NaBH_4$, NH_4OH and N_2H_5OH are given in Table 4.4.

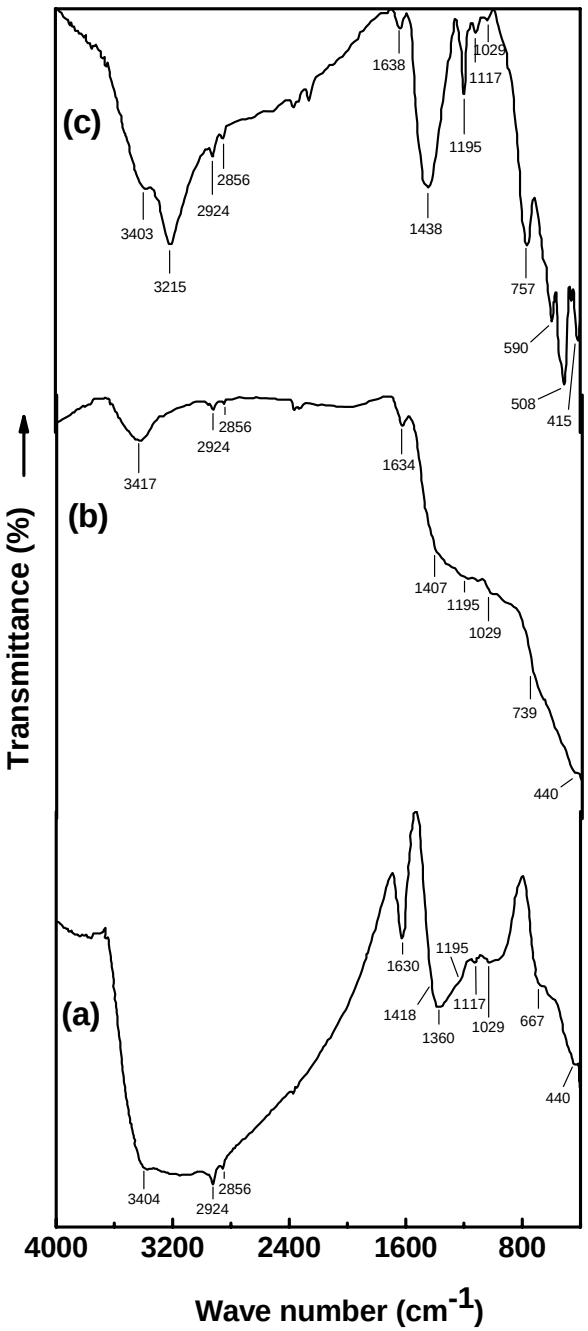

Fig. 4.10: IR spectra of (a) as-prepared ZrO_2 powder (pH 3) synthesized from $NaBH_4$ (b) calcined at 500 °C (100 % t-ZrO_2) and (c) calcined at 800 °C (100 % m-ZrO_2)

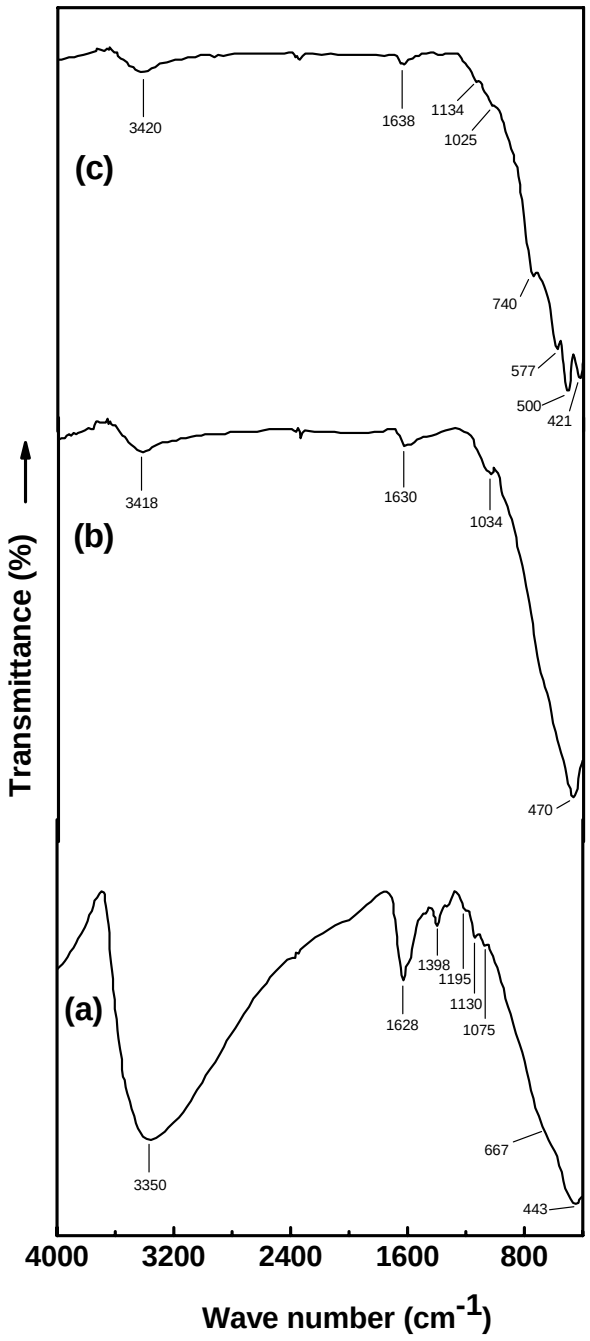

Fig. 4.11: IR spectra of (a) as-prepared ZrO_2 powder (pH 4.4) synthesized from NH_4OH (b) calcined at 500 °C (100 % t-ZrO_2) and (c) calcined at 800 °C (85 % m-ZrO_2)

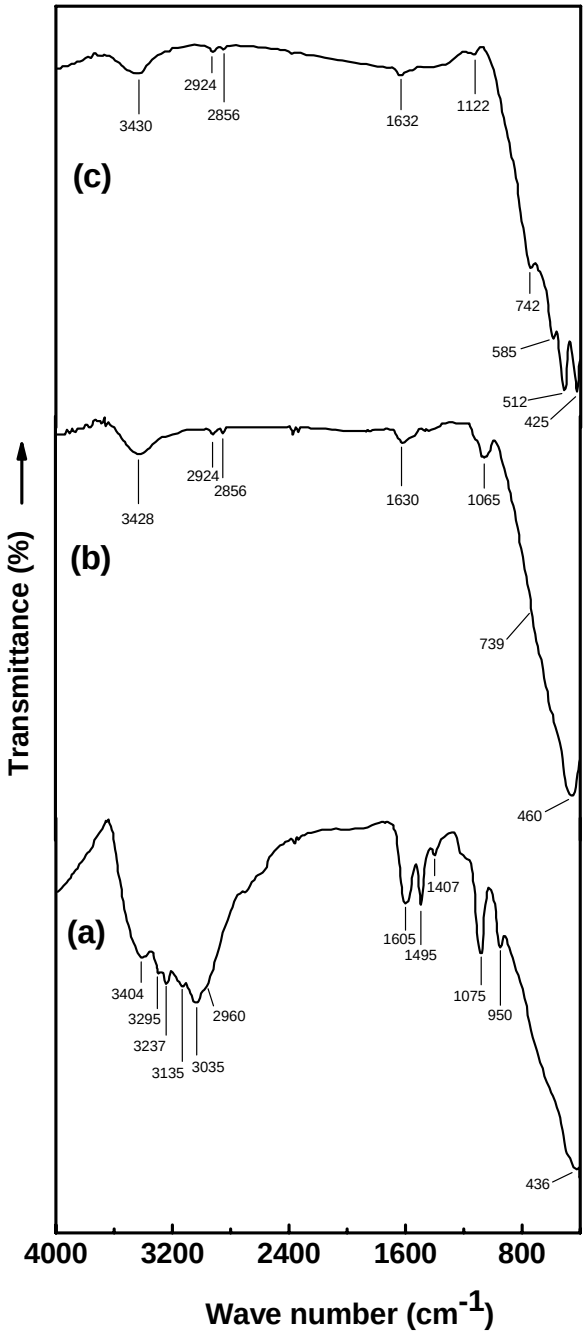

Fig. 4.12: IR spectra of (a) as-prepared ZrO_2 powder (pH 4.0) synthesized from N_2H_5OH (b) calcined at 500 °C (100 % t-ZrO_2) and (c) calcined at 950 °C (98 % m-ZrO_2)

Table 4.4: Infrared characteristic bands observed in as-prepared as well as derived *t*-ZrO_2 and *m*-ZrO_2 nanopowders

Band Position (cm^{-1}) Reaction with $NaBH_4$			
$ZrO(OH)_2.xH_2O$	*t*-ZrO_2	*m*-ZrO_2	
3404	3417	3403	O-H stretching in
		3215	$ZrO(OH)_2.xH_2O$
2924	2924	2924	or
2856	2856	2856	adsorbed water
1630	1634	1638	O-H bending in H_2O
1418	1407		O-H bending in $ZrO(OH)_2$
1360			
1195	1195	1195	
1117		1117	
1029	1029	1029	
	739	757	Zr-O vibration
667		590	
		508	
440	440	415	
Band Position (cm^{-1}) Reaction with NH_4OH			
3350	3418	3420	O-H stretching in $ZrO(OH)_2.xH_2O$ or adsorbed water
1628	1630	1638	O-H bending in H_2O
1398			O-H bending in $ZrO(OH)_2$
1195			
1130		1134	
1075	1034	1025	
		740	Zr-O vibration
667			
		577	
		500	
443	470	421	

Band Position (cm^{-1})			
	Reaction with N_2H_5OH		
3404	3428	3430	O-H stretching in $ZrO(OH)_2.xH_2O$ or adsorbed water
3295			Stretching vibration of N-N mode
3237			of
3135			Hydrazine Hydrate(N_2H_5OH)
3035			
2960	2924	2924	O-H stretching in H_2O
	2856	2856	
1605	1630	1632	O-H bending in H_2O
1495			
1407			O-H bending in $ZrO(OH)_2$
1075	1065	1122	
950			N-N stretching vibration of N_2H_5OH
	739	742	Zr-O vibration
		585	
		512	
436	460	425	

Chapter 5

CONCLUSIONS

The present work deals with the synthesis and enhancement of metastable tetragonal zirconia nanocrystals through novel chemical routes. ZrO_2 powders were synthesized through reduction and hydrolysis techniques by using a strong ($NaBH_4$), a weak (N_2H_5OH) reducing agents and a hydrolyzing (NH_4OH) agent. The significant findings of this work are:

1. The crystallization temperature of metastable t-ZrO_2 for low pH is greater as well as broader than the high pH.
2. The as-prepared powders contain lots of water in the form of $ZrO(OH)_2.xH_2O$ as studied from the IR analysis. The $ZrO(OH)_2$ is converted to t-ZrO_2 or m-ZrO_2 derivatives on heating at elevated temperatures.
3. Stabilization of metastable t-ZrO_2 is observed up to 600 °C for both pHs in case of samples reduced by $NaBH_4$.
4. Stabilization of metastable t-ZrO_2 is observed up to 500 °C for low pH in case of samples reduced by N_2H_5OH.
5. A small amount of t-ZrO_2 with major m-ZrO_2 is observed up to 950 °C for low pH. Fully m-ZrO_2 is observed from 800 °C and 1000 °C onwards for high and low pH samples respectively in case of samples reduced by N_2H_5OH.
6. Fully t-ZrO_2 is seen for low pH sample, however mixture of t- and m- ZrO_2 are observed for high pH sample up to 500 °C for the case of NH_4OH.
7. Fully m-ZrO_2 is observed after 850 °C for both pHs samples in case of NH_4OH.
8. From the XRD results it has been concluded that small crystallites (<25nm) stabilizes metastable t-ZrO_2 upto moderate temperature.
9. Low pH has better stability on metastable t-ZrO_2 compared to high pH.
10. Strong reducing agent ($NaBH_4$) gives better stability on t-ZrO_2 upto 600 °C compared to NH_4OH.
11. Reduction technique controls the crystallite size and slowly converts to m-ZrO_2 as the calcination temperature increases.
12. From the thermal as well as microstructural studies it was concluded that the stabilization of metastable t-ZrO_2 is dependent on the initial pH of the precursor, calcination temperature and also on the crystallite size of the ZrO_2.

References:

1. C. T. Lynch, F. W. Vahldiek and L. B. Robinson, J. Am. Ceram. Soc. **44**, 147 (1961).
2. R. C. Garvie, R. H. Hannink and R. T. Pascoe, Nature, **258**, 703 (1975).
3. A. H. Heuer, N. Claussen, W. M. Kriven and M. Ruhle, J. Am. Ceram. Soc., **65**, 461 (1982).
4. K. Ishida, K. Hirota, O. Yamaguchi, H. Kume, S. Inamura and H. Miymoto, J. Am. Ceram. Soc., **77**, 1391 (1994).
5. M. .Z. C. Hu, R. D. Hunt, E. A. Payzant and C.R. Hubbard, J. Am. Ceram. Soc., **82**, 2313 (1999).
6. R. H. J. Hannink, P. M. Kelly and B. C. Muddle, J. Am. Ceram. Soc., **83**, 642 (2000).
7. R. C. Garvie, J. Phys. Chem., **69**, 1238 (1965).
8. T. Yamaguchi, Catalys. Today, **20**, 199 (1994).
9. S. Stecura, Thin Solid Films, **150**, 15 (1987).
10. E. Häfele, K. Kaltenmaier and U. Schönauer, Sens. Actuat. B: Chemical, **4**, 525 (1991).
11. S. K. Pratihar, A. Dassharma and H. S. Maiti, Mater. Res. Bul., **40**, 1936 (2005).
12. A. S. Carrillo, T. Tagawa and S. Goto, Mater. Res. Bull., **36**, 1017 (2001).
13. A. S. Carrillo, T. Tagawa and S. Goto, C. Z. Huang, L. Zhang, L. He, H. L. Liu, J. Sun, B. Fang, Z. Q. Li and X. Ai, J. Mater. Proc. Techn., **129**, 349 (2002).
14. K. Morita, K. Hiraga and B. -N. Kim, Act. Mater., **52**, 3355 (2004).
15. Z. Wang, D. Tao, G. Guo, S. Jin, F. Wei, W. Qian, S. Hong and J. Guo, Mater. Lett., **60**, 3104 (2006).
16. A. C. Dodd and P. G. McCormick, J. Euro. Ceram. Soc., **22**, 1823 (2002).
17. J. Liang, X. Jiang, G. Liu, Z. Deng, J. Zhuang, Fuli Li and Yadong Li, Mater. Res. Bull. **38**, 161 (2003).
18. L. Li and W. Wang, Sol. Stat. Commun., **127**, 639 (2003).
19. Y. V. Kolen'ko, V. D. Maximov, A. A. Burukhin, V. A. Muhanov and B. R. Churagulov, Mater. Sc. Eng: C, **23**, 1033 (2003).

20. Y. L. Zhang, X. J. Jin, Y. H. Rong, T. Y. Hsu (X. Zuyao), D. Y. Jiang and J. L. Shi, Mater. Sc. Eng.: A, **438-440**, 399 (2006).

21. M. I. Osendi, J. S. Moya, C. J. Serna and J. Soria, J. Am. Ceram. Soc., **68**, 135 (1985).

22. R. Srinivasan, L. Rice and B. H. Davis, J. Am. Ceram. Soc., **73**, 3528 (1990).

23. N. Igawa, Y. Ishii, T. Nagasaki, Y. Morii, S. Funahashi and H. Ohno, J. Am. Ceram. Soc., **76**, 2673 (1993).

24. N. Igawa and Y. Ishii, J. Am. Ceram. Soc., **84**, 1169 (2001).

25. K. Bandyopadhyay, S. R. Sainkar and K. Vijayamohanan, J. Am. Ceram. Soc., **82**, 222 (1999).

26. F. J. Berry, S. J. Skinner, L. N. Bell, R. J. H. Clark and C. B. Ponton, J. Sol. State. Chem., **145**, 394 (1999).

27. B. Xia, L. Duan, Y. Xie, J. Am. Ceram. Soc., **83**, 1077 (2000).

28. N. L. Wu and T. F. Wu, J. Am. Ceram. Soc., **83**, 3225 (2000).

29. A. Mondal, S. Ram, J. Am. Ceram. Soc., **87**, 2187 (2004).

30. M. H. Lee, H. Y. Lin and J. L. Thomas, J. Am. Ceram. Soc., **89**, 3624 (2006).